From underdoped to overdoped cuprates: two quantum phase transitions

Sergey G. Ovchinnikov[1, 2], Elena I. Shneyder[1, 3], Maxim M. Korshunov[1, 4, *]

The mystery of high temperature superconductivity in layered cuprates is tightly related to their common patter of the doping-dependent evolution from the antiferromagnetic insulator at zero doping to the overdoped metal. A number of experimental and theoretical studies indicate that the evolution is not smooth and a critical point separates the underdoped (UD) and overdoped (OD) regions. It is tempting to associate such critical point with the pseudogap formation for $p < p*$, with $p^* = 0.19 \div 0.24$ [1-3]. No doubt that the proximity of the pseudogap and the superconductivity with two energy scales, T^* and T_c, is essential for high-T_c superconductivity [4]. On the other hand, the Hall effect measurements suggest that the critical point and the quantum phase transition (QPT) take place at optimal doping, $p_{opt} = 0.16$ [5]. To resolve this controversy, here we performed precise density of states calculations and found that there are *two* QPTs and the corresponding critical concentrations associated with the change of the Fermi surface topology upon doping.

Angle-resolved photo-emission spectroscopy (ARPES) reveals a change of the Fermi surface (FS) topology from the small hole pockets to the large hole FS near the optimal doping [6, 7]. This provides a link between the QPT and changes of the FS. Here we will apply the general Lifshitz ideas [8] on the QPT induced by the FS transformations. But first of all, we will discuss how these transformations are induced by doping.

It is easy to obtain the large FS in cuprates by a single-electron approach like the local density approximation (LDA) or the tight-binding method. However, to get the small hole pockets around the $(\pm\pi/2, \pm\pi/2)$ points of the Brillouin zone requires going beyond the weak-coupling approximations and taking the strong electronic correlations into account. Such small pockets have been found in a doped antiferromagnetic (AFM) Mott insulator by exact diagonalization [9] and Quantum Monte Carlo [10] calculations for the finite clusters as well as by a perturbation treatment of the infinite lattice [11-13]. According to these studies, after the long-range AFM order vanishes with increasing hole concentration $n_h = 1 + p$ (in $La_{2-x}Sr_xCuO_4$, $p = x$) a short-range AFM order still persists even at optimal doping [14]. The short-range magnetic order determines the self-energy and hole dispersion resulting in the small hole pockets around the $(\pm\pi/2, \pm\pi/2)$ points in the UD cuprates, its fluctuation results in the pseudogap formation [15-17]. Due to the strong electronic correlations intrinsic for cuprates a theory of the electron dynamics has to fulfill a "no-double occupancy" constraint. This constraint is introduced explicitly in the mean-field theory of a d-type superconductivity within the RVB approach for the $t-J$ model [18], and in the variational Monte-Carlo studies [19].

Contrary to the phenomenological approaches, like assuming that the second order QPT exists at $p = p_c$ [20], we deal with a microscopically derived $t - t' - t'' - J^*$ model without free parameters. All parameters, including intraband t_{fg}^{11} and interband t_{fg}^{12} hoppings, have been calculated within a hybrid LDA+GTB approach [21], which combines the *ab initio* LDA and the

[1]*Institute of Physics, Siberian Branch of RAS, Krasnoyarsk, 660036, Russia*
[2]*Siberian Federal University, Krasnoyarsk, 660041, Russia*
[3]*Siberian Aerospace University, Krasnoyarsk, 660014, Russia*
[4]*Department of Physics, University of Florida, Gainesville, Florida 32611, USA*
* E-mail : korshunov@phys.ufl.edu

generalized tight-binding (GTB) method for strongly correlated systems. Both short-range magnetic order and "no-double occupancy" constraint are incorporated in our approach by the Hubbard X-operators perturbation theory, which was developed earlier for $p-d$ [22, 23] and $t-J$ [24, 25] models. The method of irreducible Green functions used in this theory is similar to the Mori-type projection technique, with the zero-order Green function given by the well-known Hubbard I approximation. Beyond it there are spin fluctuations. To provide a description of them, the self-energy was calculated in the noncrossing approximation by neglecting vertex renormalization that is equivalent to the self-consistent Born approximation (SCBA) [23]. Resulting electron self-energy contains the space-time dependent spin correlation function. Note that at low temperatures $T \le 10\,K$ the spin dynamics is much slower than the electron one. A typical spin fluctuation time, 10^{-9} sec, is much larger than the electronic time 10^{-13} sec [26]; that is why we can safely neglect the time dependence of the spin correlation function. The self-energy becomes static, $\sum(\mathbf{k},\omega) \to \sum(\mathbf{k})$, and is determined by static spin correlation function $C_{0n} = \left\langle S_0^+ S_n^- \right\rangle$ and kinetic correlation function $K_{0n} = \sum_\sigma \left\langle c_{0\sigma}^\dagger c_{n\sigma} \right\rangle$ between sites 0 and n (see the methods section). These correlation functions and their Fourier transforms $C_{\mathbf{q}}$ and $K_{\mathbf{q}}$ represent the AFM short-range order and the valence bond order, respectively. A self-consistent calculation of these functions up to $n = 9$ (ninth coordination sphere) together with the chemical potential as functions of doping x reveals that all C_{0n} decrease with doping. While the nearest neighbor spin correlation function C_{01} is finite for all studied x up to $x = 0.40$ with a kink at $x = p^* = 0.24$, more distant spin correlations fall down to zero for $x > p^*$.

The calculated FS twice changes its topology with doping [25]. Small hole pockets around $(\pm\pi/2, \pm\pi/2)$ points are present at small doping; then they increase in size and touch each other in the non-symmetric points $\mathbf{k} = \pm\pi(1, \pm 0.4)$ at $x_{c1} = p_{opt} = 0.151$. Above p_{opt}, there are two Fermi surfaces around (π,π) with outer being a hole-like and inner being an electron-like. The electron Fermi surface collapsed at $x_{c2} = p^* = 0.246$, and at $x > p^*$ we have only one large hole surface around (π,π). Similar conclusion on the coexistence of hole and electron FS at some intermediate doping have been also drawn recently [27, 28].

From the previous consideration it follows that the FS topological transitions in cuprates are induced by doping and they are due to the non-rigid band behaviour of the quasiparticles in the strongly correlated systems. According to the general Lifshitz analysis [8], for the three dimensional (3D) system a change of topology at the energy $\varepsilon = \varepsilon_c$ either by appearance of a new segment (like we found at p^*) or by change of its connectivity (like at p_{opt}) would result in the additional density of states, $\delta N(\varepsilon) \sim (\varepsilon - \varepsilon_c)^{1/2}$, and the change in the thermodynamic potential, $\delta\Omega \sim (\varepsilon_F - \varepsilon_c)^{5/2}$ (the QPT of the 2.5-order), where ε_F is the Fermi energy. However, due to the strong anisotropy of electronic and magnetic properties, cuprates are quasi-2D and not isotropic 3D systems. The electron hopping perpendicular to the CuO_2 layers in a single-layer $La_{2-x}Sr_xCuO_4$ (LSCO), $Bi_2Sr_2CuO_{6+\delta}$ (Bi2201), etc. is negligibly small. We do not consider here $YBa_2Cu_3O_{7-\delta}$ (YBCO) and $Bi_2Sr_2CaCu_2O_{8+\delta}$ (Bi2212) with two CuO_2 layers in the unit cell where the bilayer splitting of the Fermi surface appears, so we calculate the density of states (DOS) for the electrons in the doped single CuO_2 layer.

The change of the FS topology at $x_{c1} = p_{opt}$ results in the logarithmic divergence of DOS (Fig. 1), while the emergence of the new electron-like pocket below $x_{c2} = p^*$ results in a step in DOS (Fig. 2). The total DOS is a sum of the singular and regular contributions. We would like to

stress that both log and step DOS singularities are in perfect agreement with the general properties of the van Hole singularities for the 2D electrons. Contrary to the 3D systems, the thermodynamical potential for the 2D electrons has a singular contribution $\delta\Omega \sim \left(\varepsilon_F - \varepsilon_c\right)^2$ for the step singularity and $\delta\Omega \sim \left(\varepsilon_F - \varepsilon_c\right)^2 \ln\left|\varepsilon_F - \varepsilon_c\right|$ for the log singularity [29]. Thus QPT at $x_{c2} = p^*$ is of the second order, while at $x_{c1} = p_{opt}$ the singularity is stronger. It is immediately follows that the Sommerfeld parameter γ in the electronic heat capacity $\gamma = C_e/T$ has also a singular step contribution at $x \le p^*$, and $\delta\gamma \propto \ln\left(\varepsilon_F - \varepsilon_c\right) \propto \ln\left|x - x_{opt}\right|$ near $x_{c1} = p_{opt}$.

To check whether the coincidence of x_{c1} with p_{opt} and x_{c2} with p^* is occasional or not we have calculated the superconducting critical temperature dependence $T_c(x)$ in the same model [30] and the kinetic energy as a function of doping. The $T_c(x)$ dependence is an inverse parabola with the maximum at x_{opt} (see inset in Fig. 1), which indeed equal to x_{c1}. Note that it is not a coincidence since like in the BCS theory the maximum in $T_c(x)$ is determined by the maximum density of states, and at x_{c1} we have a log singularity. Kinetic energy,

$$E_{kin} = \sum_n t_{0n}^{11} K_{0n}\,, \qquad (1)$$

reveals a remarkable kink at $x_{c2} = p^*$ (Fig. 3). Above p^*, $E_{kin}(p)/E_{kin}(p^*) \approx 1 + p$ that is expected for a conventional 2D metal with hole concentration $n_h = 1 + p$ and $E_{kin} \sim \varepsilon_F \sim n_h$. The extrapolation of this law below p^* (shown in Fig. 3 by the blue dashed line) reveals that actual E_{kin} is smaller. We associate this depletion of the kinetic energy with the pseudogap formation and try to fit it with a simple free electron gas with a triangular pseudogap DOS (Loram-Cooper model [1]):

$$N(\varepsilon) = \begin{cases} g, & \left|\varepsilon - \varepsilon_F\right| > E_g \\ g\,\dfrac{\left|\varepsilon - \varepsilon_F\right|}{E_g}, & \left|\varepsilon - \varepsilon_F\right| < E_g \end{cases}. \qquad (2)$$

Here $E_g = J\left(p^* - p\right)/p^*$ is a doping dependent pseudogap, J is the exchange parameter. This fitting is shown by the filled triangles and it reflects some decrease of the kinetic energy due to the pseudogap but do not provide a quantitative agreement. Apparently, better fitting is given by the exponentional law,

$$E_{kin}(p)/E_{kin}(p^*) = \exp\left\{-4E_g(p)/J\right\}. \qquad (3)$$

Anyway, this analysis confirms that the QPT at x_{c2} is indeed related to the pseudogap and the coincidence of x_{c2} and p^* is not occasional.

A singular contribution to the Hall coefficient near the optimal doping has been measured for $Bi_2Sr_{0.51}La_{0.49}CuO_{6+\delta}$ single crystals and for $La_{2-x}Sr_xCuO_4$ thin films [5] under strong magnetic field of 60T. According to our theory, these extra carriers are induced by the singular DOS. To continue discussion in terms of the critical points, not the critical energies, we note that near the critical point $\varepsilon_F(x) - \varepsilon_{c1} = k\left(x - x_{opt}\right)$. In Fig. 4 we plot the calculated singular DOS $N_{\text{sing}}(z)$, $z = x - x_{opt}$, together with the singular contribution to the Hall coefficient, $n_{Hall}(1.5K) - n_{Hall}(100K)$ [5]. The optimal doping in the LSCO thin film $x_{opt} = 0.17$ is shifted from the bulk value $x_{opt} = 0.15$ in the Bi2201 which may be due to the strains in the films. The general agreement of the calculated singular DOS and Hall data provides further support for our analysis.

In summary, we have shown that there are *two* critical points in the cuprate's doping dependence. The first one is related to the change of the FS connectivity and logarithmic divergences of DOS and of electronic heat capacity parameter γ at the optimal doping $p_{opt} = 0.151$. Also, we associate this QPT with the experimentally observed singular doping dependence of the Hall coefficient [5]. Moreover, the logarithmic enhancement of DOS leads to the maximum in the doping dependence of superconducting critical temperature T_c at the same critical point $x = p_{opt}$. This is in agreement with the previous calculations of T_c for the magnetic mechanism of $d_{x^2-y^2}$ pairing. The second QPT is associated with the collapse of the electron-like FS pocket at $p \to p^* = 0.246$ and results in the step singularities in DOS and in Sommerfeld parameter γ. We have found the depletion of the hole's kinetic energy below p^* and ascribe it to the pseudogap formation at $p < p^*$. Thus the two energy scales in cuprates measured by T_c and T^* are both related to the QPTs and evolution of the cuprate's electron structure with doping. The very existence of both logarithm and step singularities in DOS are in perfect agreement with the general properties of the van Hole singularities for the 2D electron systems. But the concentrations of doping at which these singularities approach the Fermi level and start to govern the behavior of the system are determined by the strong electronic correlations and scattering on the associated short-range AFM order.

"Methods"

To properly fulfill the "no-double occupancy" constraint at every step of our calculations we use the Hubbard X-operators, $X^{pq} = |p\rangle\langle q|$, where $|p\rangle$ and $|q\rangle$ are the local eigenvectors corresponding to three states: one-hole state $|\sigma\rangle$, $\sigma = \pm 1/2$, and the Zhang-Rice singlet, $|S\rangle$, which is a two-hole (zero-electron) state. Constraint results in the exclusion of two-electron (zero-hole) state $|0\rangle = d^{10}p^6$ from the local Hilbert space. In the Hubbard model, there are two fermions with spin σ: $X^{0\sigma}$ and $X^{\bar{\sigma}S}$ $(\bar{\sigma} \equiv -\sigma)$, forming the lower (LHB) and the upper (UHB) Hubbard bands. In the hole representation the LHB corresponds to an empty conduction band of electrons and the UHB corresponds to a valence band. The "no-double occupancy" constraint means the absence of the direct excitations from and to the LHB; the doped holes occupied only the UHB. Nevertheless the virtual interband (between the LHB and the UHB) hopping t^{12} results in the exchange interaction $J_{fg} = \left(t_{fg}^{12}\right)^2 / U_{\text{eff}}$. For $La_{2-x}Sr_xCuO_4$, all intraband and interband hopping parameters (t_{fg}^{11} and t_{fg}^{12}), single-site energies of holes in p- and d-orbitals, and the charge transfer gap U_{eff} have been calculated by the *ab initio* LDA+GTB method [10]. The low energy effective model is the $t-t'-t''-J^*$ model where J^* means that besides the Heisenberg exchange term a three-site correlated hopping H_3 is also included. In terms of the Hubbard X-operators the Hamiltonian $H_{t-J^*} = H_{t-J} + H_3$ is given by

$$H_{t-J} = \sum_{f,\sigma}(\varepsilon-\mu)X_f^{\sigma\sigma} + \sum_f 2(\varepsilon-\mu)X_f^{SS} + \sum_{f\neq g,\sigma} t_{fg}^{11} X_f^{S\bar{\sigma}} X_g^{\bar{\sigma}S} + 1/4 \sum_{f\neq g,\sigma} J_{fg}\left(X_f^{\sigma\bar{\sigma}} X_g^{\bar{\sigma}\sigma} - X_f^{\sigma\sigma} X_g^{\bar{\sigma}\bar{\sigma}}\right), \quad (4)$$

$$H_3 = \sum_{f\neq m\neq g,\sigma} \frac{t_{fm}^{12} t_{mg}^{12}}{U_{\text{eff}}}\left(X_f^{S\bar{\sigma}} X_m^{\sigma\sigma} X_g^{\bar{\sigma}S} - X_f^{S\sigma} X_m^{\sigma\bar{\sigma}} X_g^{\bar{\sigma}2}\right).$$

Here hole creation operator is now $c_\sigma^\dagger = 2\sigma X^{S\bar{\sigma}}$ and its algebra is different from the bare fermion's one. The spin operators are also easily expressed via X-operators, $S^+ = X^{\sigma\bar{\sigma}}$, $S^z = \left(X^{\sigma\sigma} - X^{\bar{\sigma}\bar{\sigma}}\right)/2$. The self-energy calculated in the SCBA [23] is determined by the spin correlation function $C(q,\omega)$ and results in the finite quasiparticle lifetime, $\text{Im}\Sigma(k,E) \neq 0$. As

discussed above, at low temperatures we can neglect spin dynamics, $C(q,\omega)\to C_{\mathbf{q}}$, and then we have $\mathrm{Im}\Sigma=0$. Nevertheless the doping evolution of the Fermi surface is determined by the $\mathrm{Re}\Sigma$, and it is qualitatively similar in our approach [25] and in the approach which properly takes $\mathrm{Im}\Sigma$ into account [23]. The Green function for a hole moving against the background of short-range AFM order is written as

$$G(\mathbf{k},E)=\left\langle\left\langle X_{\mathbf{k}}^{\bar{\sigma}2}\middle|X_{\mathbf{k}}^{2\bar{\sigma}}\right\rangle\right\rangle_{E}=\left[E-(\varepsilon_0+U_{\mathrm{eff}}-\mu)-\frac{1+x}{2}t_{\mathbf{k}}-\frac{1-x^2}{4}\frac{\tilde{t}_{\mathbf{k}}^2}{U_{\mathrm{eff}}}+\Sigma(\mathbf{k})\right]^{-1}\frac{1+x}{2} \tag{5}$$

where

$$\begin{aligned}\Sigma(\mathbf{k})=&-\frac{2}{1+x}\frac{1}{N}\sum_{\mathbf{q}}\left[t_{\mathbf{k}-\mathbf{q}}-\frac{(1-x)}{2}J_{\mathbf{q}}+\frac{(1-x)}{2}\frac{\tilde{t}_{\mathbf{k}-\mathbf{q}}^2}{U_{\mathrm{eff}}}-\frac{(1+x)}{2}\frac{2\tilde{t}_{\mathbf{k}}\tilde{t}_{\mathbf{k}-\mathbf{q}}}{U_{\mathrm{eff}}}\right]\frac{3}{2}C_{\mathbf{q}}\\&-\frac{2}{1+x}\frac{1}{N}\sum_{\mathbf{q}}\left[t_{\mathbf{q}}-\frac{(1-x)}{2}J_{\mathbf{k}-\mathbf{q}}-x\frac{\tilde{t}_{\mathbf{q}}^2}{U_{\mathrm{eff}}}-\frac{(1+x)}{2}\frac{2\tilde{t}_{\mathbf{k}}\tilde{t}_{\mathbf{k}-\mathbf{q}}}{U_{\mathrm{eff}}}\right]K_{\mathbf{q}}.\end{aligned} \tag{6}$$

Here, $t_{\mathbf{k}}$ and $\tilde{t}_{\mathbf{k}}$ are the Fourier transforms of hoppings t_{fg}^{11} and t_{fg}^{12}, respectively. In contrast to approach of Ref. 23, we calculate correlation functions $C_{\mathbf{q}}$ and $K_{\mathbf{q}}$ self-consistently together with the chemical potential. To get the spin correlation function we also obtain the spin-spin Green function $\left\langle\left\langle X_{\mathbf{q}}^{\sigma\bar{\sigma}}\middle|X_{\mathbf{q}}^{\bar{\sigma}\sigma}\right\rangle\right\rangle_{\omega}$ in a spherically-symmetric spin liquid state [24] with $\langle S^z\rangle=0$ and the equal correlation functions for each spin component, $\langle S_0^+S_n^-\rangle=2\langle S_0^zS_n^z\rangle=C_{0n}$. Both C_{0n} and K_{0n} are essentially doping-dependent [25].

It should be stressed that the standard DOS calculations with routine precision (400×400 points in the quarter of BZ) we used before to solve the T_c equation for magnetic mechanism of $d_{x^2-y^2}$ -wave pairing [30] is not enough to find the effect of QPT on DOS. To get the results presented here we used $10^5\times10^5$ k -points which lead to the increase of precision by 625 times.

Acknowledgements

This work is supported by the Russian Foundation for Basic Research, Grant N 09-02-00127, by the Integration Program of SBRAS N40, the Presidium RAS Program 5.7, and in part by the National Science Foundation under Grant NSF PHY05-51164.

References

1. Loram, J. W., Luo, J., Cooper, J. R., Liang, W. Y., Tallon, J. L. Evidence on the pseudogap and condensate from the electronic specific heat. *J. Phys. Chem. Solids* **62**, 59-64 (2001).
2. Castellani, C., Di Castro, C., Grilli, M., Non-Fermi-liquid behavior and d-wave superconductivity near the charge-density-wave quantum critical point *Z. Phys. B* **103**, 137-144 (1997).
3. Daou, R. et al. Linear temperature dependence of resistivity and change in the Fermi surface at the pseudogap critical point of a high-T_c superconductor. *Nature Physics*, **5**, 31-34 (2009).
4. Hüfner, S., Hossain, M. A., Damascelli, A., Sawatzky, G. A. Two gaps make a high-temperature superconductor? *Rep. Prog. Phys.* **71**, 062501 (2008).

5. Balakirev, F. F. et al. Quantum Phase Transition in the Magnetic-Field Induced Normal State of Optical-Doped High-T_c Cuprate Superconductors at Low Temperatures. *Phys. Rev. Lett.* **102**, 017004 (2009).
6. Damacelli, A., Hussein, Z., Shen, Z.X., Angle-resolved photoemission studies of the cuprate superconductors. *Rev. Mod. Phys.* **75**, 473 (2003).
7. Meng, J. et al. Direct Observation of Fermi Pocket in High Temperature Cuprate Superconductors. arXiv:0906.2682 (2009).
8. Lifshitz, I. M., Azbel, M. Y., Kaganov, M. I. Electron theory of Metals. Consultant Press, New York, 1972. *JETP* **11**, 1130-1145 (1960).
9. Stephan, W., Horsh, P. Fermi surface and dynamics of the t-J model at moderate doping *Phys. Rev. Lett.* **66**, 2258-2261 (1991).
10. Preuss, R., Hanke, W., von der Linden, W. Quasiparticle Dispersion of the 2D Hubbard Model: From an Insulator to a Metal. *Phys. Rev. Lett.* **75**, 1344-1347 (1995).
11. Shraiman, B. I., Siggia, E. D. Mobile Vacancies in a Quantum Heisenberg Antiferromagnet. *Phys. Rev. Lett.* **61**, 467-470 (1988).
12. Trugman, S. A. Explanation of Normal-State Properties of High-Temperature Superconductors. *Phys. Rev. Lett.* **65**, 500-503 (1991).
13. Chen, W. Q., Yang, K. Y., Rice, T. M., Zhang, F. C. Quantum oscillations in magnetic-field-induced antiferromagnetic phase of underdoped cuprates: application to ortho-II $YBa_2Cu_3O_{6.5}$. *Europhys. Lett.* **82**, 17004 (2008).
14. Thurston, T. R., Birgeneau, R. J., Kastner, M. A., and Preyer, N. W. Neutron scattering study of the magnetic excitations in metallic and superconducting $La_{2-x}Sr_xCuO_{4-y}$. *Phys. Rev. B.* **40**, 4585-4595 (1989).
15. Kampf, A. P. Magnetic correlations in high temperature superconductivity. *Physics Reports* **249**, 222-340 (1994).
16. Schmalian, J., Pines, D., Stojkovic, B. Microscopic theory of weak pseudogap behaviour in the undoped cuprate superconductors: General theory and quasiparticle properties. *Phys. Rev. B* **60**, 667-686 (1999).
17. Kuchinskii, E. Z., Sadovskii, M. V. Models of the Pseudogap State of Two-Dimensional Systems. *JETP* **88,** 968- (1999).
18. Baskaran, G., Zhou, Z., Anderson, P. W. The resonating valence bond state and high-T_c superconductivity — A mean field theory. *Sol. St. Communs.* **63**, 973-976 (1987)
19. Pathak, S. et al. Competition between Antiferromagnetic and Superconducting States, Electron-Hole Doping Assymetry, and Fermi-Surface Topology in High Temperature Superconductors. *Phys. Rev. Lett.* **102**, 027002 (2009).
20. Senthil, T. Critical Fermi surfaces and non-Fermi liquid metals. *Phys. Rev. B.* **78**, 035103 (2008).
21. Korshunov, M. M. et al. Hybrid LDA and generalized tight-binding method for electronic structure calculation of strongly correlated electron systems. *Phys. Rev. B* **72**, 165104 (2005).
22. Barabanov, A. F., Kovalev, A. A., Urazaev, O. V., Belmuk, A. M., and Hayn, R. Evolution of the Fermi surface of cuprates within spin-polaron approach. *JETP* **92**, N4, 677-695 (2001).
23. Plakida, N. M., Oudovenko, V. S. Electron spectrum in high-temperature cuprate superconductors *JETP* **104**, N2, 230-244 (2007).
24. Val'kov, V. V., Dzebisashvili, D. M. The electron Energy Spectrum and Superconducting Transition Temperature of Strongly Correlated Fermions with Three-Center Interactions. *JETP* **100**, N3, 608-617 (2005).
25. Korshunov, M. M., Ovchinnikov, S. G. Doping dependent evolution of low-energy excitations and quantum phase transitions within an effective model for high-T_c copper oxides. *Eur. Phys. J. B* **57**, 271-278 (2007).

26. Harrison, N., Mc Donald, R. D., Singleton, J., Cupate Fermi Orbits and Fermi Arcs: The Effect of Short-Range Antiferromagnetic Order. *Phys. Rev. Lett*. **99**, 206406 (2007).
27. Hozoi, L., Laad, M. S., Fulde, P. Fermiology of cuprates from first principles: From small pockets to the Luttinger Fermi surface. *Phys. Rev. B* **78**, 165107 (2008).
28. Chakravarty, S., Kee, H.-Y. Fermi pockets and quantum oscillations of the Hall coefficient in high-temperature superconductors. *Proc. Nat. Acad. Sc. (USA)* **105**, 8835-8839 (2008).
29. Nedoresov, S. S. Surface effects in the thermodynamics of conductivity electrons. *JETP* **23**, 1124-1130 (1966).
30. Shneyder, E. I., Ovchinnikov, S. G. Phonon and magnetic pairing mechanisms in high-T_c temperature superconductors in the strong correlation mode. *JETP Lett.* **83**, 394-398 (2006).

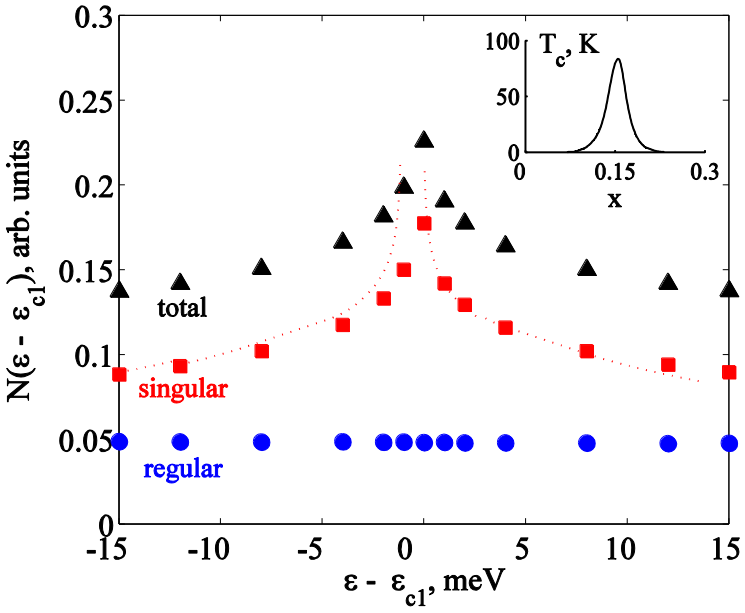

Fig. 1. Regular, singular, and total density of states $N(\varepsilon-\varepsilon_{c1})$ near the optimal doping $\varepsilon_{c1}=\varepsilon_F(p_{opt})$ as calculated from the Green function (5). Dotted line shows the log fitting. In the inset, the doping dependence of the superconducting critical temperature $T_c(x)$ is shown; the optimal doping is 0.151.

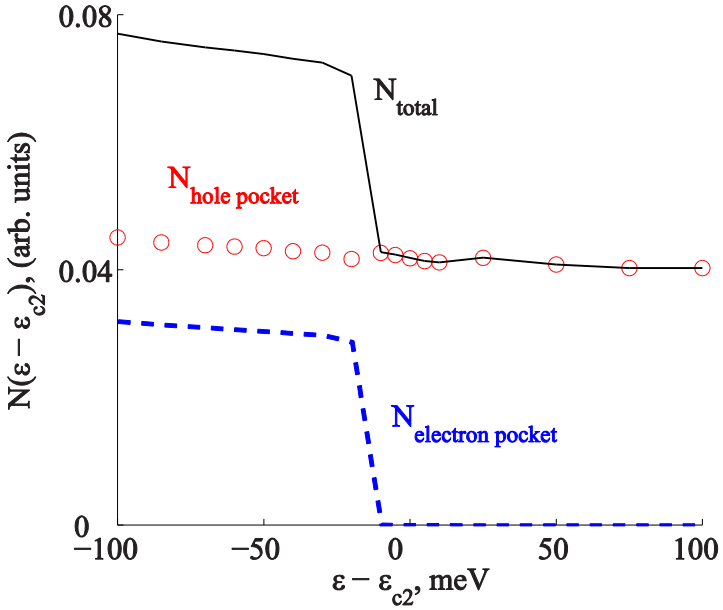

Fig. 2. Regular (hole pocket), singular (electron pocket), and total density of states $N(\varepsilon-\varepsilon_{c1})$ near the pseudogap critical point $\varepsilon_{c2}=\varepsilon_F(p^*)$. Below $p^*=0.24$ $(\varepsilon<\varepsilon_{c2})$ a singular step-like contribution to the total DOS appears.

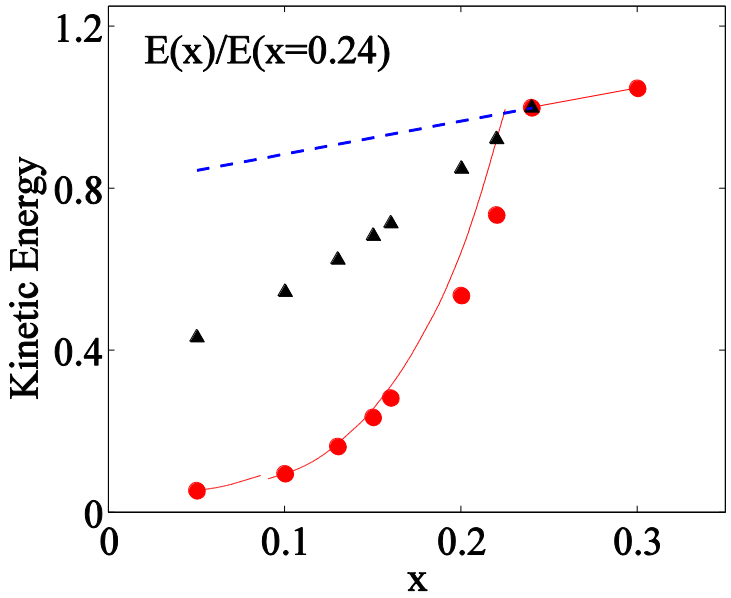

Fig. 3. The doping dependence of the dimensionless kinetic energy $E_{kin}(p)/E_{kin}(p^*)$**.** Calculated dependence shown by the filled red circles. Above p^* it obeys a conventional law and proportional to $(1+p)$. The extrapolation of this law to the region $p < p^*$ (blue dashed line) emphasizes the depletion of part of the kinetic energy in the pseudogap region. Calculation for the idealized triangular pseudogap model (2) is shown by the filled triangles.

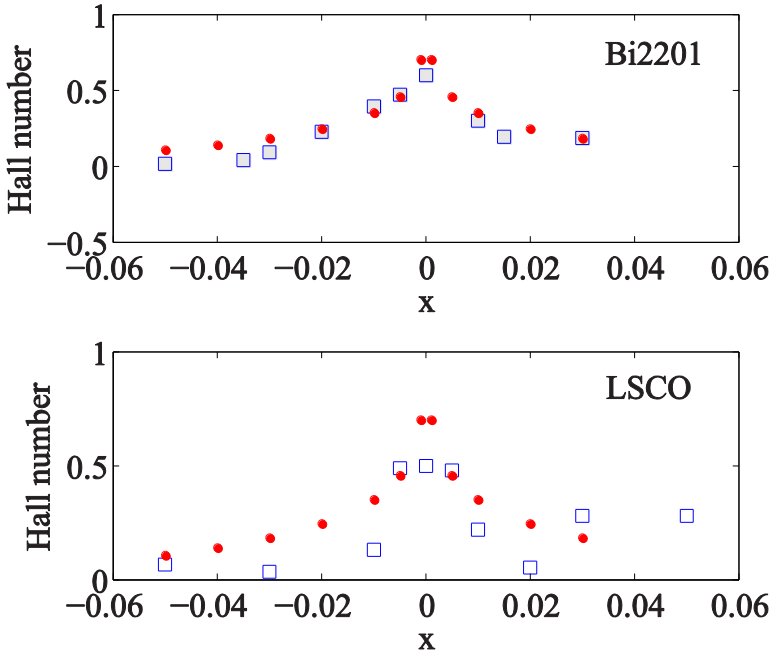

Fig. 4. Comparison of experimental singular Hall coefficient [5] for $Bi_2Sr_{0.51}La_{0.49}CuO_{6+\delta}$ **(a) and for** $La_{2-x}Sr_xCuO_4$ **(b) and our calculated singular DOS** $N_{\text{sing}}\left(\varepsilon_F(x)\right)$ **near the optimal doping.** Agreement with results on bulk single crystals (a) is better than with results on thin films (b).